Rev Bras Cardiol Invasiva.
2014;22(3):203-15

Original Article

Edge Dissections After the Coronary Implantation of Bioresorbable Scaffolds. Serial Analysis Using Optical Coherence Tomography

Daniel Chamié[1], Evandro M. Filho[1], Fábio Grandi[2], Ricardo A. Costa[1], J. Ribamar Costa Jr.[1], Dimytri Siqueira[1], Rodolfo Staico[1], Fausto Feres[1], Andrea Abizaid[1], Luiz Fernando Tanajura[1], Amanda G.M.R. Sousa[1], Alexandre Abizaid[1]

ABSTRACT

Background: The incidence of edge dissections after the coronary implantation of bioresorbable scaffolds (BRS) has not been investigated. BRS have thicker struts and require more aggressive pre-dilation for implantation. The incidence of edge dissections after BRS implantation, their morphological aspects and healing process were evaluated using serial optical coherence tomography (OCT) images. **Methods**: Consecutive patients treated with a polymeric BRS, who had an OCT evaluation after the procedure and at 6-month follow-up, were included in the current analysis. Edge dissections were defined as luminal surface ruptures, 5-mm distally or proximally to the BRS edges. **Results**: Out of 96 edges from 48 BRS implanted in 48 lesions of 48 patients, 91 edges were available for analysis. Dissections were detected by OCT in 28 edges (30.7%) and in 22 lesions (45.8%), with equal distribution between distal and proximal edges. All dissections appeared as flaps and none were visible by angiography. Atherosclerotic disease was present in 96.4% of all dissected edges; most were fibrocalcific (40.8%), and more than one-third were lipid-rich. Mean dissection length was 1.80 mm, and the mean flap area was 0.30 mm. Most dissections (89.3%) were superficial and restricted to the intima/atheroma layer. At the 6-month follow-up 92.8% of all dissections healed completely, and there was no significant reduction in the luminal dimensions at the edge segments, with only one case of restenosis. **Conclusions**: Edge dissections are frequent after polymeric BRS implantation. Dissections, only detected by OCT, were short in length, superficial, were not flow-limiting, and presented favorable clinical outcomes.

DESCRIPTORS: Percutaneous coronary intervention. Stents. Tomography, optical coherence. Absorbable implants. Coronary restenosis.

RESUMO

Dissecções de Borda Após Implante Coronário de Suportes Vasculares Biorreabsorvíveis. Análise Seriada com Tomografia de Coerência Óptica

Introdução: A incidência de dissecções de borda, após o implante de suportes vasculares biorreabsorvíveis (SVBs), ainda não foi investigada. Esses suportes têm hastes mais espessas e requerem pré-dilatação mais agressiva no implante. Avaliamos a incidência de dissecções de borda após implante de SVBs, seus aspectos morfométricos e o processo de cicatrização, com imagens de tomografia de coerência óptica (OCT) seriadas. **Métodos**: Incluímos pacientes consecutivos, que foram tratados com SVBs polimérico, e que possuíam avaliação com OCT após o procedimento e aos 6 meses de evolução. Dissecções de borda foram definidas como rupturas da superfície luminal nos 5 mm distais ou proximais ao SVB. **Resultados**: Das 96 bordas de 48 SVB implantados em 48 lesões de 48 pacientes, 91 bordas estavam disponíveis para a análise. Dissecções foram detectadas pela OCT em 28 bordas (30,7%) de 22 lesões (45,8%), com igual distribuição entre as bordas distais e proximais. Todas as dissecções apareceram como flaps e não foram visualizadas pela angiografia. Doença aterosclerótica esteve presente em 96,4% das bordas dissecadas; a maioria era fibrocalcificada (40,8%) e mais de um terço era rica em lipídio. O comprimento médio das dissecções foi 1,80 mm e a área média dos flaps tinha 0,30 mm. A maioria das dissecções (89,3%) era superficial, restrita à camada íntima/ateroma. No seguimento de 6 meses, 92,8% das dissecções cicatrizaram e não houve redução significativa nas dimensões luminais nos segmentos de borda, com apenas um caso de reestenose. **Conclusões**: Dissecções de borda são frequentes após implante de SVBs poliméricos. As dissecções, apenas detectadas pela OCT, foram curtas, superficiais, sem comprometimento do fluxo coronário e apresentaram evolução clínica favorável.

DESCRITORES: Intervenção coronária percutânea. Stents. Tomografia de coerência óptica. Implantes absorvíveis. Reestenose coronária.

[1] Instituto Dante Pazzanese de Cardiologia, São Paulo, SP, Brazil.
[2] Cardiovascular Research Center, São Paulo, SP, Brazil.

Correspondence to: Daniel Chamié. Serviço de Cardiologia Invasiva do Instituto Dante Pazzanese de Cardiologia – Avenida Dr. Dante Pazzanese, 500 – Vila Mariana – CEP: 04012-180 – São Paulo, SP, Brazil
E-mail: daniel.chamie@gmail.com

Received on: 06/11/2014 • Accepted on: 08/28/2014

Plaque fracture and arterial-wall dissection are the main mechanisms by which luminal gain is obtained during balloon angioplasty and stent implantation.[1,2] In the case of stents, plaque dissections are "sealed" by the device mesh along the treated segment. However, lesion in the transition from their rigid structure with the vessel wall may occur and be associated with increased risk of major adverse cardiac events (MACE).[3-7]

Registries with intravascular ultrasound (IVUS) reported incidences of edge dissections after coronary stenting ranging from 5% to 23%.[8] Optical coherence tomography (OCT) is an invasive imaging modality that provides tomographic images of the coronary vessel with axial resolution between 10 and 15 microns (ten times the resolution provided by IVUS),[9] allowing for a detailed evaluation of the vascular microstructure and stent/vessel interaction. Consequently, the incidence of edge dissections detected by OCT tends to be higher than those described in angiography and IVUS studies. In fact, in the largest series published to date, edge dissections were detected by OCT in 37.8% of 249 lesions treated with drug-eluting stent (DES) in a daily clinical practice population.[10]

The introduction of bioresorbable scaffolds (BRS) requires different implantation strategies from those usually used for metal stents, namely: (1) identify the proximal and distal references to the target lesion that have the highest lumen dimensions and morphological appearance closest to normal and less atherosclerotic disease on angiography, preventing the implantation of the BRS when there is a caliber disproportion > 0.75 mm between the distal and proximal references; (2) accurate length measurement between the proximal and distal references to the target lesion, aiming to optimize the choice of device length, so that its edges are positioned on the site with less distal disease and proximal to the treated lesion; (3) a "more aggressive" pre-dilation with use of non-compliant balloon catheter aiming at a balloon-artery ratio of 1:1, in addition to residual stenosis < 40%; (4) gradual inflation of the BRS with increments of two atmospheres of pressure every 10 seconds; and (5) a "less aggressive" post-dilation (if necessary) with non-compliant balloon catheters, with a maximum diameter of 0.5 mm, larger than the nominal diameter of the implanted BRS.

It is not yet known whether this approach results in increased occurrence of edge dissections after BRS implantation. While greater care regarding case selection, the implant, and the post-dilation of the device may result in less injury to edge segments, pre-dilation with larger-caliber balloons and greater thickness of the device struts (~ 150 µm) can have the opposite effect.

In the present study, we used OCT to assess the incidence of edge dissections after implantation of polymeric BRS, describe their qualitative and quantitative morphometric aspects, and the evolution of its healing process, with serial images 6 months after the index procedure.

METHODS

Population and study design

The present study included patients with single coronary lesions who were treated with the DESolve® BRS (Elixir Medical Corporation, Santa Clara, United States) and underwent evaluation with OCT after the procedure and at the end of 6 months.

Inclusion criteria consisted in the presence of a single, *de novo* coronary lesion, with angiographic stenosis diameter > 50% and evidence of myocardial ischemia. The target vessel had to have a reference diameter between 2.75 and 3.0 mm, and the lesions could not be longer than 12 mm in length. The main exclusion criteria were: myocardial infarction < 72 h, severe left ventricular dysfunction (left ventricular ejection fraction – LVEF < 30%), lesions located in the left main coronary artery or involving important side branches (> 2.0 mm), restenotic lesions, and the presence of thrombus or calcification identified by angiography.

Device used in the study

The DESolve BRS consists of a polymer platform based on poly-L-lactic acid (PLLA) with 150 µm thick struts. The device is covered by a matrix of polylactic acid, which carries and releases the antiproliferative drug novolimusat at a dose of 5 µg/mm. Novolimus is an active metabolite of sirolimus and belongs to the family of macrocyclic lactones inhibitors of the Mtor enzyme. Approximately 85% of the drug is released within 4 weeks. The polylactic acid matrix that carries and releases the drugs is bioreabsorbed within 6 to 9 months, while the device polymeric base is bioreabsorbed between the first and second years.

Intervention procedure

Pre-treatment with a loading dose of acetylsalicylic acid (300 mg) and clopidogrel (300 or 600 mg) was administered to patients who were not on chronic use of these medications. At the start of the procedure, anticoagulation with unfractionated heparin (100 IU/kg) was performed with administration of additional boluses, whenever necessary to maintain an activated clotting time ≥ 250 seconds. Glycoprotein IIb/IIIa inhibitors were used according to the surgeon's discretion. Pre-dilation of the target lesion with non-compliant balloon, aiming at a balloon:artery ratio of 1:1, was mandatory. The implantation of the BRS DESolve was performed with gradual insufflation using increments of two atmospheres of pressure every 10 seconds until a ratio of 1:1 had been achieved with the reference vessel

diameter. Post-dilation was performed at the surgeon's discretion and, when performed, it had to be carried out with non-compliant balloons with a diameter up to 0.5 mm larger than the nominal diameter of the implanted BRS.

No formal recommendation was given regarding the management of dissections identified by OCT, and the decision to treat was entirely the surgeon's responsibility. If the implantation of an additional stent was required, a commercially available metallic DES with thin struts, releasing a drug of the "-limus" family, was to be used.

Angiographic analysis

All angiograms were analyzed independently for the study of edge dissections, with the examiner blinded to the findings obtained from the OCT analysis.

When present, the magnitude and severity of the dissection were graded according to the classification of the National Heart, Lung, and Blood Institute in types A to F.[11] The final epicardial coronary flow was graded according to the Thrombolysis In Myocardial Infarction criteria (TIMI) from zero to 3.[12]

Acquisition and image analysis of optical coherence tomography

OCT images were acquired with a commercially available Fourier-Domain OCT system (C7-XR® OCT Intravascular Imaging System; St. Jude Medical, St. Paul, United States). After intracoronary administration of nitroglycerin (100-200 µg), a conventional 0.014 – coronary – angioplasty guide wire was positioned in the distal bed of the target vessel, and the imaging catheter (DragonFly®; St. Jude Medical, St. Paul, United States) was advanced over the guide wire and positioned at least 10 mm distally to the distal edge of BRS to be investigated. During intracoronary iodinated contrast injection through an injector pump (8 to 16 mL injected at a velocity of 3 to 6 mL/s, 300 psi), a 54 mm scan of the coronary vessel was performed with automatic pullback of the OCT catheter at a velocity of 20 mm/s. All images were stored in digital media and sent for analysis at an independent core lab (Cardiovascular Research Center, São Paulo, Brazil).

All images were carefully evaluated regarding their quality. Edges with less than 5 mm in length, or cases with poor vascular wall visualization due to artifacts or the presence of large amount of residual blood, were excluded from analysis.

The borders that delimit the beginning and end of the BRS were defined by the first and last frames in which the BRS struts were displayed in all four quadrants of the image. The regions comprising 5 mm distal and proximal to the BRS borders were defined as the segments of the distal and proximal edge, respectively (Figure 1). Edge dissections were defined as ruptures of the luminal vessel surface in the BRS edge segments, identified in at least two consecutive frames. Dissections were morphologically classified as flaps or cavities (Figure 2).[10] To quantify the magnitude of the dissection, the authors used previously described morphometric parameters (Figure 3).[10] The severity of each dissection was also evaluated qualitatively regarding the depth of vascular injury as: (1) intimal, a dissection limited to the intimal layer of the vessel or atheroma; (2) medial, a dissection extending up to the medial layer of the vessel; and (3) adventitial, a dissection extending to the vessel external elastic membrane.[13] In cases where the medial layer was not visible, the dissection was classified as intimal. Presence of intramural hematoma was defined as an accumulation of blood (or contrast medium) in the medial space, displacing the intimal internally and the external elastic membrane externally (Figure 2C).[13] Intraluminal thrombus was characterized as a mass with irregular borders adhered to luminal surface or fluctuating inside the lumen.

The presence or absence of atherosclerotic disease at the site where the BRS edges were placed at implantation was also investigated. A typical vessel was characterized by the presence of trilaminar architecture,[13] with intimal thickening < 250 µm.[14] If the BRS edges had been placed in a site with atherosclerotic disease, the type of underlying plaque was characterized as fibrotic, fibrocalcific, or lipid-rich, as previously described.[13,15] In lipid plaques, its longitudinal and circumferential distribution and the mean and minimum thickness of

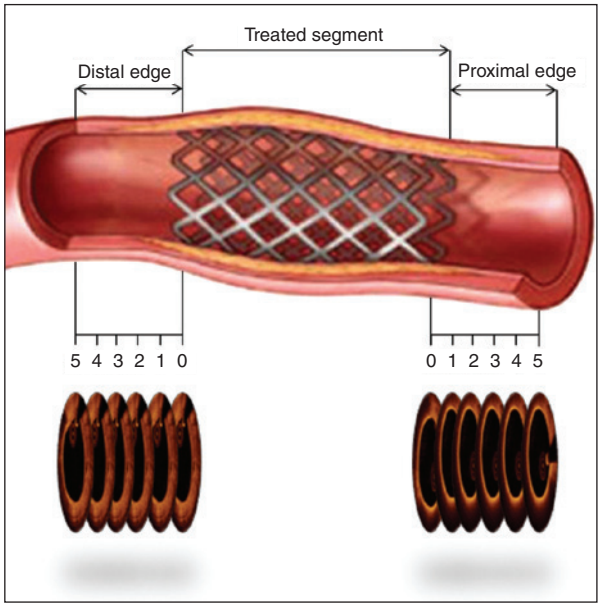

Figure 1 – Definition of the analysis' segments. The regions comprising 5 mm distal and proximal to the vascular bioresorbable scaffold limits were defined as the distal and proximal edge segments, respectively.

Rev Bras Cardiol Invasiva.
2014;22(3):203-15

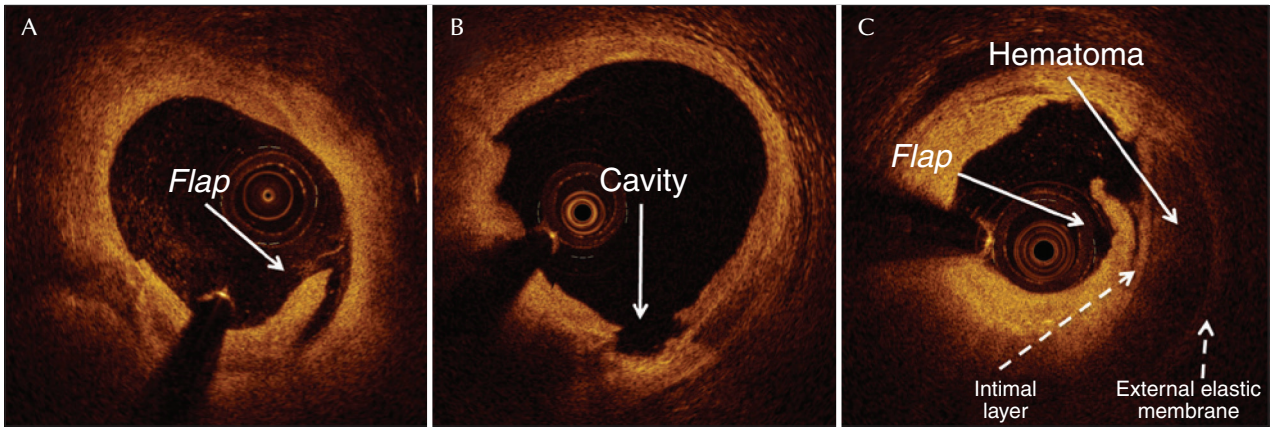

Figure 2 – Morphology of dissections. (A) Flap dissections; (B) cavities; (C) intramural hematoma, defined as a collection of blood (or contrast medium) within the medial space, displacing the intimal layer internally and the external elastic membrane externally.

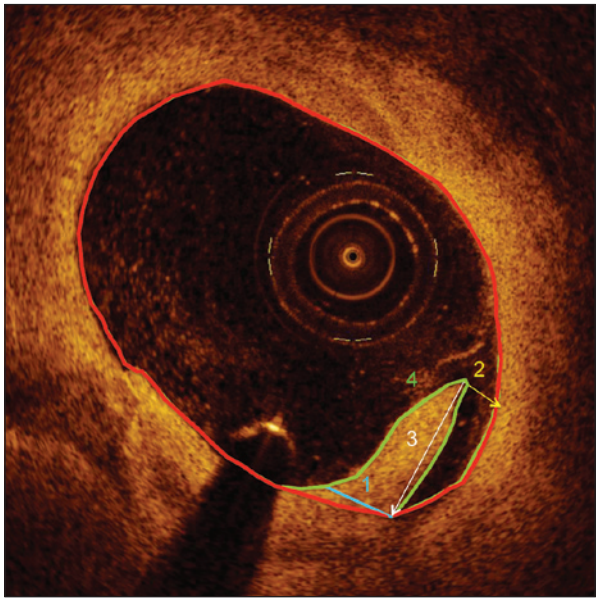

Figure 3 – Morphometric flap assessment. Morphometric parameters were used to quantify the dissection magnitude: (1) flap depth, thickness of the flap base; (2) flap opening, distance between the tip of the flap and the luminal contour; (3) flap length, distance between the tip of the flap and its point of junction with the luminal contour; and (4) flap area, measured by planimetry from the external contour of the flap.

the protective fibrous cap were quantified. A thin-cap fibroatheroma was defined as a lipid-rich plaque with minimal fibrous cap thickness < 65 μm.

All analyses were performed using an off-line proprietary analysis program (OCT System Software B.0.1, St. Jude Medical, St. Paul, United States). All evaluations described above were performed in all consecutive frames along the edge segments (interval between images of 0.2 mm), while quantitative measurements of vascular lumen area and diameters were performed at every millimeter.

Statistical analysis

All statistical analyses were performed using SPSS, version 20.0 (IBM Corp., Armonk, United States). Continuous variables were presented as means and standard deviations, and categorical variables as frequencies and percentages. Serial analyses were performed with the nonparametric Friedman's test (two-way analysis of variance by ranks) or Wilcoxon's test (Wilcoxon signed-rank test). Two-tailed values of $p < 0.05$ were considered as statistically significant.

RESULTS

Incidence of edge dissections detected by optical coherence tomography

In total, 48 patients (48 lesions) treated with the DESolve BRS underwent evaluation with OCT after the index procedure. Of the 96 possible edges, 2 distal and 3 proximal edges were not visualized. Consequently, 91 edges were available for analysis (46 distal and 45 proximal), in 48 lesions of 48 patients. Edge dissections were detected by OCT in 28 edges (30.7%) of 22 lesions (45.8%) in 22 patients (45.8%). The dissections were equally distributed between distal (14/46; 30.4%) and proximal edges (14/45; 31.1%). Six lesions in six patients had dissections in both edges. The flowchart presents the number of patients in the sample, lesions, and edges included in the study, as well as the reasons for exclusion of edges that were not analyzed (Figure 4).

Clinical and procedural characteristics

The clinical and procedural characteristics of the 22 patients in whom edge dissections were identified

by OCT are shown in tables 1 and 2, respectively. The mean age was 62.9 ± 7.5 years; 59.1% of patients were males and 18.2% were diabetics. The clinical picture that led to coronary intervention was stable angina in most patients (86.4%).

The left anterior descending artery was the most frequently treated vessel (41%). The treated lesions were relatively short (11.36 ± 3.20 mm). Pre-dilation was performed in all cases. The mean diameter and the length of the implanted BRS were 3.09 ± 0.15 mm and 15.45 ± 1.97 mm, respectively. Post-dilation was performed in only 27% of cases, with maximum balloon pressure of 14.8 ± 4.8 atm. The mean balloon:artery ratio in all cases was 1.12 ± 0.10.

None of the dissections detected by the OCT was identified by angiography, and TIMI flow 3 was obtained after the procedure in all cases.

Characterization of the plaque type in edge segments of the bioresorbable scaffold by optical coherence tomography

Among the 28 edges with dissection, only one showed no atherosclerotic disease. Table 3 shows the incidence of the types of atherosclerotic plaque on which the edges of the BRS were positioned. Fibrocalcific plaques accounted for the majority (40.8%) of the plaques in dissected edges, while approximately one-third of the edges (33.3%) had lipid-rich plaques. Importantly, seven (77.7%) of the nine lipid plaques were located on the proximal edges, and these accounted for 50% of all types of plaques in the dissected proximal edges. In the quantification of all lipid plaques, the mean thickness of protective fibrotic caps was 286.8 μm, while the mean minimal thickness was 145.5 μm. Only one lipid plaque in a distal edge showed minimal fibrous cap thickness of 60 μm (< 65 microns), meeting the criteria to be characterized as a thin-cap fibroatheroma.

Morphometric evaluation of edge dissections by optical coherence tomography

Table 4 shows the morphometric assessment of dissections, overall and individually, according to the location of the edges. The values of the previously published morphometric analysis of 106 dissections identified by OCT after metallic DES implantation, analyzed with the same methodology applied in this study, are presented only so that the current findings can be put into perspective. The mean length of the dissections was 1.80 mm and all presented as flaps; 1.43 flaps were identified by dissection; 12 (3.6%) dissections had more than one flap visible. The maximum flap opening measured 0.17 mm with an area of 0.30 mm. Most (89.3%) dissections were restricted to

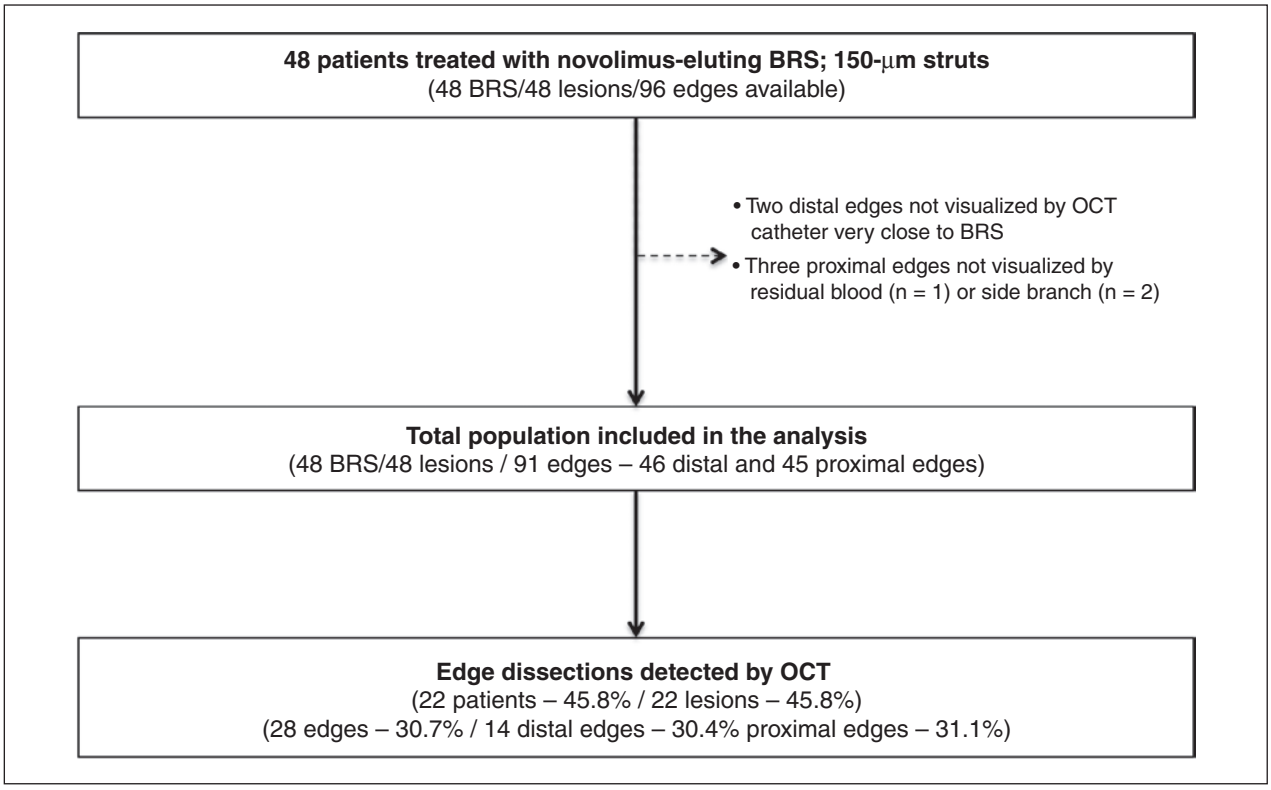

Figure 4 – Study flowchart. Population selected for inclusion and cases excluded from the analysis, as well as incidence of dissections, according to different levels (for instance: patient, lesion, and edge). OCT: optical coherence tomography; BRS: bioresorbable scaffold.

TABLE 1
Baseline clinical characteristics

	n = 22 patients
Age, years	62.9 ± 7.5
Male gender, n (%)	13 (59.1)
Arterial hypertension, n (%)	16 (72.7)
Dyslipidemia, n (%)	4 (18.2)
Current smoking, n(%)	15 (68.2)
Previous infarction, n (%)	14 (63.6)
Previous PCI, n (%)	5 (22.7)
PCI indication, n (%)	
Stable angina	19 (86.4)
Unstable angina	3 (13.6)

PCI: percutaneous coronary intervention.

TABLE 2
Angiographic and procedure characteristics

	n = 22 lesions
Target vessel, n (%)	
Left anterior descending artery	9 (41)
Left circumflex artery	7 (32)
Right coronary artery	6 (27)
Lesion length, mm	11.36 ± 3.20
Reference vessel diameter, mm	2,97 ± 0.34
Minimal luminal diameter, mm	0.91 ± 0.38
Stenosis diameter, %	69.4 ± 12.2
Pre-dilation, n (%)	22 (100)
BRS nominal diameter, mm	3.09 ± 0.15
BRS nominal length, mm	15.45 ± 1.97
Post-dilation, n(%)	6 (27)
Maximum inflation pressure, atm	14.8 ± 4.8
Balloon:artery ratio	1.12 ± 0.10

BRS: bioresorbable scaffold.

the intimal/atheroma layer of the vessel, with only three (10.7%) dissections extending to the medial layer. No deep dissections that extended to the vessel external elastic membrane were observed. Intramural hematoma was identified in only one proximal dissection, with a length of 1.1 mm and a maximal area of 0.66 mm. Intraluminal thrombi were not observed in any dissected edge. Although dissections located in the distal edge showed a tendency to be longer (2.14 ± 1.36 mm vs. 1.11 ± 0.76 mm; p = 0.11), there were no significant morphometric differences in the dissections located at the distal edges in comparison with those located in the proximal edges.

Serial assessment of dissected edges by optical coherence tomography

All 28 dissected edges had serial OCT images at 6 months of follow-up. After this period, 26 (92.8%) dissections were completely healed, with no trace of edge lesion visualized at the 6 month evaluation (Figure 5). Table 5 shows the morphometric characteristics of the two dissections that persisted after 6 months. It is noteworthy that both were superficial (extending up to the intimal/atheroma layer) and located in the distal edges, and presented a significant reduction in their dimensions.

It should be highlighted that no significant reduction was observed in luminal area and diameter of the distal and proximal edges during the 6 months of evolution (Figure 6). One dissection at the proximal edge of an implanted BRS developed restenosis and required reintervention (Figures 6 and 7).

Clinical follow-up

In the clinical follow-up of six months, the occurrence of MACE was 4.5%. There were no cases of death or myocardial infarction, and only one case of reintervention due to restenosis at the proximal edge of a BRS was observed. This patient had a dissection in the distal and proximal edges of a 3.0 × 14 mm BRS implanted in the left circumflex artery. At 6 months of follow-up, this patient had stable class II angina with documented myocardial ischemia on stress testing. Assessment with OCT showed that the dissection located at the distal edge was still present and that the proximal edge, despite showing a completely healed dissection, developed a significant post-procedure reduction of luminal area, from 3.80 mm^2 to 1.57 mm^2. Due to the presence of angina and documentation of ischemia, the patient underwent a new intervention with implantation of a metallic DES.

DISCUSSION

This study is the first investigation on the incidence of edge dissections after implantation of polymeric BRS. In addition to the high-resolution images provided by OCT, a systematic methodology was used to quantify in detail the extent and magnitude of vascular injury in edge segments and performed a serial evaluation of dissection evolution over 6 months. The main findings were: (1) lesions in edge segments are often visualized by OCT after BRS implantation; (2) the dissections assessed here were small, did not limit coronary flow, and were mostly superficial (89.3%); (3) the incidence of atheroma in vascular segments, in which the BRS edges were placed, was high (96.4%), although they

TABLE 3
Characterization of plaque type in edge segments

	Total (n = 28)	Distal edges (n = 14)	Proximal edges (n = 14)	*p*-value*
Edge characteristics, n (%)				> 0.99
Normal vessel	1 (3.6)	1 (7.1)	0	
Presence of atherosclerotic plaque	27 (96.4)	13 (92.9)	14 (100)	
Plaque type, n (%)				0.16
Fibrotic	7/27 (25.9)	5/13 (38.5)	2/14 (14.3)	
Fibrocalcified	11/27 (40.8)	6/13 (46.1)	5/14 (35.7)	
Lipid-rich	9/27 (33.3)	2/13 (15.4)	7/14 (50.0)	
Quantification of lipid-rich plaques	n = 9	n = 2	n = 7	
Longitudinal length, mm	2.23 ± 1.34	3.20 ± 2.54	1.95 ± 0.96	0.61
Fibrous-cap mean tickness, µm	286.8 ± 114.4	178.0 ± 67.9	317.8 ± 107.8	0.12
Fibrous-cap minimal thickness, µm	145.6 ± 60.4	70.0 ± 14.1	167.1 ± 48,9	< 0.01
TCFA, n(%)	1 (11.1)	1 (50)	0 (0)	N/A

* *p*-value corresponds to the comparison between distal and proximal edges. TCFA: thin-cap fibroatheroma; N/A: not applicable.

TABLE 4
Morphometric assessment of edge dissections by optical coherence tomography

	Total (n = 28)	Distal edges (n = 14)	Proximal edges (n = 14)	*p*-value*	Dissections of metallic DES (n = 106)†
Dissection length, mm	1.80 ± 1.17	2.14 ± 1.36	1.11 ± 0.76	0.11	2.04 ± 1.60
Dissection morphology, n (%)				N/A	
Flap	28 (100)	14 (100)	14 (100)		102 (96.2)
Cavity	0	0	0		13 (12.3)
Number of flaps per dissection	1.43 ± 0.50	1.44 ± 0.52	1.27 ± 0.46	0.55	1.45 ± 0.77
Maximum flap depth, mm	0.42 ± 0.26	0.51 ± 0.35	0.40 ± 0.24	0.60	0.62 ± 0.39
Maximum flap opening, mm	0.17 ± 0.11	0.18 ± 0.10	0.12 ± 0.06	0.15	0.39 ± 0.34
Maximum flap length, mm	0.94 ± 0.62	0.58 ± 0.37	0.99 ± 0.93	0.46	1.09 ± 0.67
Flap area, mm^2	0.30 ± 0.34	0.29 ± 0.26	0.34 ± 0.50	0.37	0.39 ± 0.39
Dissection depth, n(%)				0.54	
Intimal layer/atheroma	25 (89.3)	13 (92.9)	12 (85.7)		50 (47.2)
Medial layer	3 (10,7)	1 (7,1)	2 (14.3)		51 (48.1)
Adventitial layer	0 (0)	0 (0)	0 (0)		5 (4.7)
Intramural hematoma, n (%)	1 (3.6)	0 (0)	1 (7.1)	N/A	10 (9.4)
Intraluminal thrombus, n (%)	0 (0)	0 (0)	0 (0)	N/A	4 (3.8)

*p-value corresponds to the comparison between distal and proximal edges; †Adapted from Chamie et al.[10] DES: drug-eluting stent; N/A: not applicable.

appeared to be normal at the angiography; (4) most (92.8%) of the dissections healed completely over the course of 6 months, without excessive tissue formation, with only one patient developing restenosis; (5) the clinical evolution of patients with edge dissections seen only by OCT, with no coronary flow impairment, was uneventful in the in-hospital phase, with only one case of repeated revascularization after 6 months. There were no cases of acute myocardial infarction or stroke associated with the dissections.

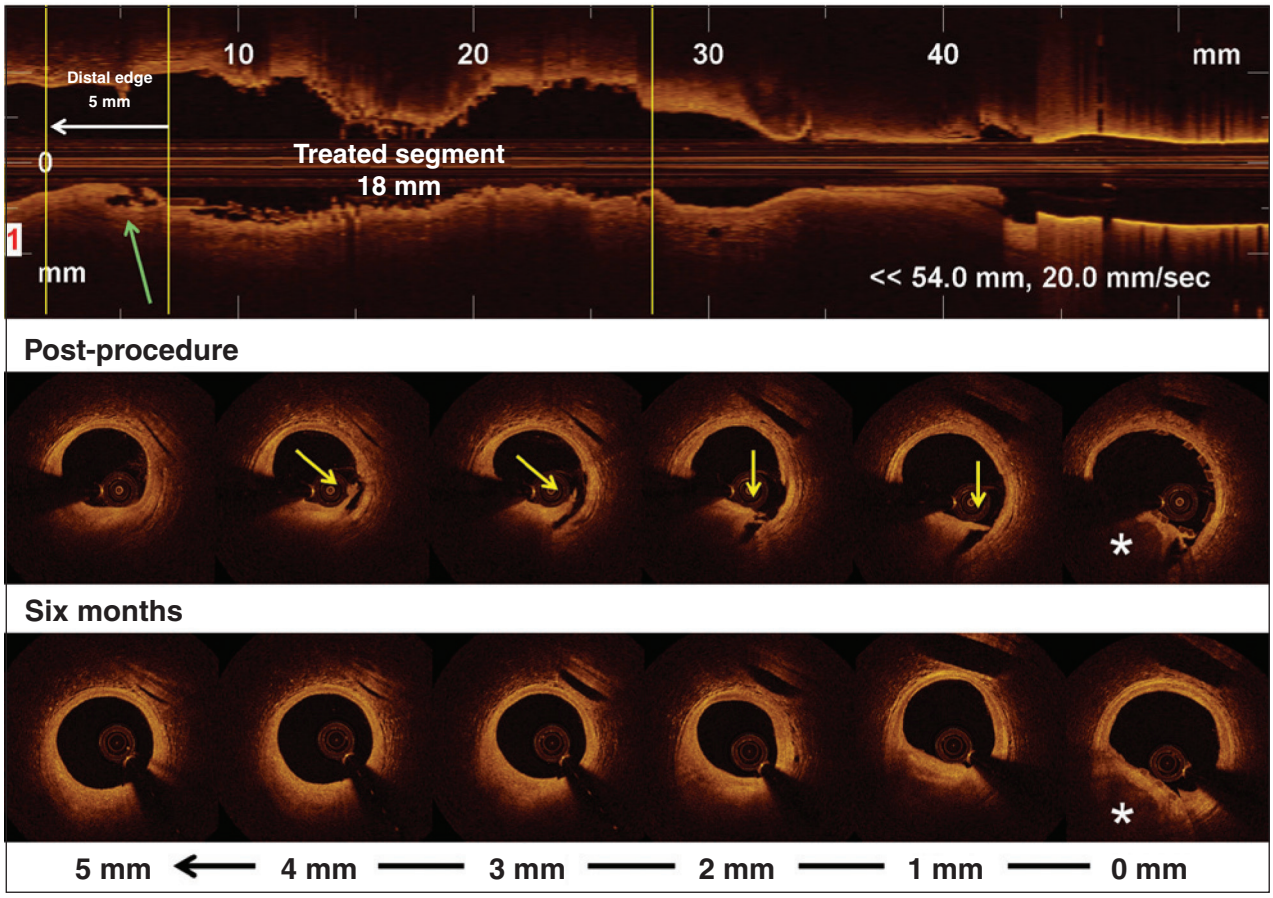

Figure 5 – Example of healed edge dissection. Top panel shows a longitudinal view of optical coherence tomography after the implantation of the bioresorbable scaffold. The treated segment, as well as the 5 mm from the distal edge, is delimited by the vertical yellow lines. Observe the dissection segment at the distal edge of the bioresorbable scaffold (green arrow). The middle panel shows cross-sectional images along the 5 mm from the distal edge. Observe the long dissection with flap morphology (yellow arrows). The bottom panel shows cross-sectional images along the 5 mm from the distal edge corresponding to the regions shown in the middle panel. Observe the complete healing of the dissection with restoration of smooth luminal contour and without irregularities. The pericardium structure visible at 1 o'clockhelps in co-recordingimages after the procedure (middle panel) and after 6 months (bottom panel). The white asterisks show an eccentric calcified plaque, over which the edge of the bioresorbable scaffold was positioned.

TABLE 5
Serial evaluation of edge dissections that persisted at the end of 6 months

	Dissection 1		Dissection 2	
	Post-procedure	6 months	Post-procedure	6 months
Longitudinal length, mm	2.7	0.5	4.1	1.6
Dissection depth	Intimal	Intimal	Intimal	Intimal
Maximal flap depth, mm	0.94	0.50	0.19	0.25
Maximal flap opening, mm	0.12	0.30	0.37	0.10
Maximal flap length, mm	1.29	0.79	1.50	0.59
Flap area, mm^2	0.57	0.21	0.46	0.14

Incidence of edge dissections

Edge dissections after coronary stenting have been reported in 1.7 to 6.4% of cases by angiography,[3,6] with an incidence ranging from 5 to 23% when the percutaneous coronary intervention outcome was assessed with IVUS.[8,16] In a recent analysis,[10] the authors investigated, through OCT, 395 edges of metallic DES

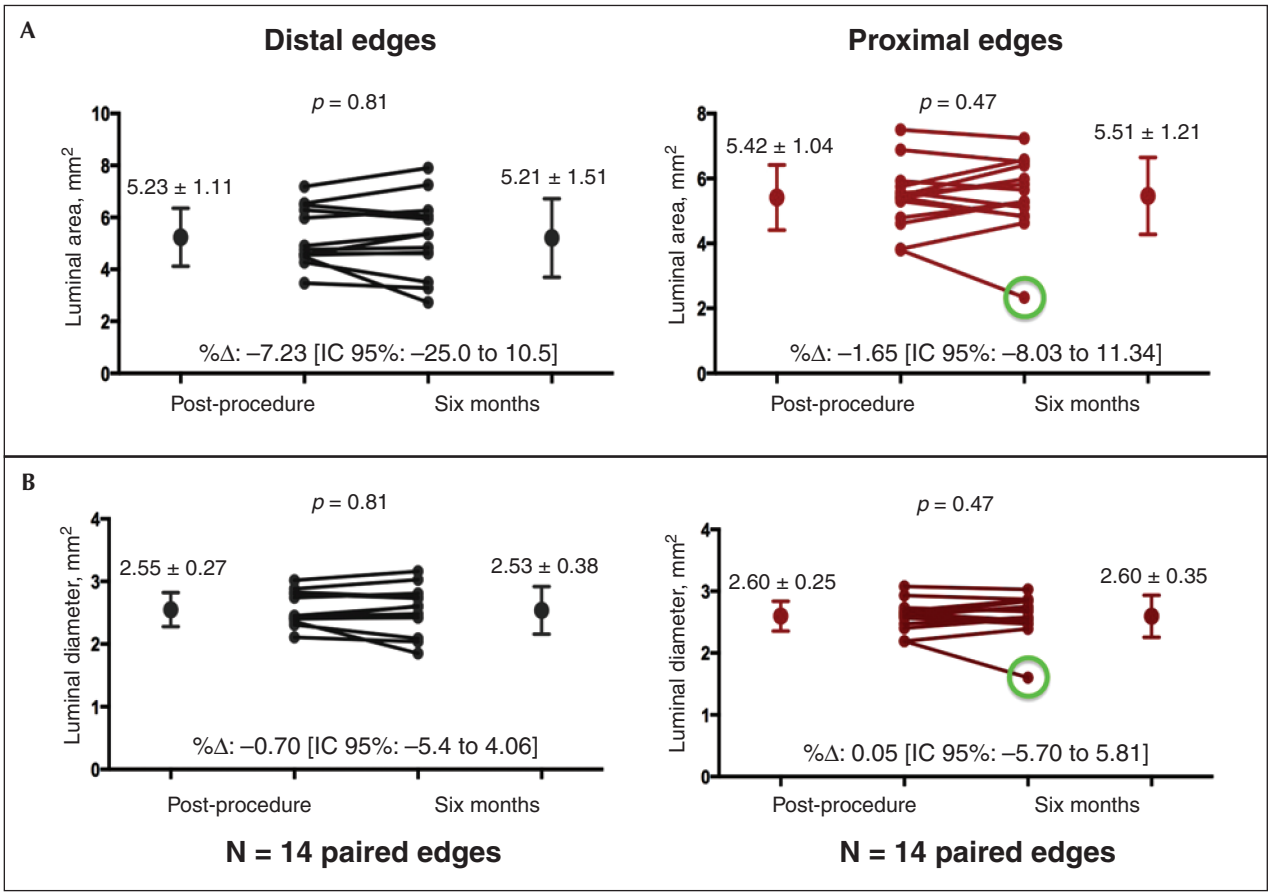

Figure 6 – Change in luminal dimensions by optical coherence tomography of the dissected edges between post-procedure period and after 6 months. (A) Change in luminal area between post-procedure periodand after 6 months in the distal (black lines) and proximal edges (red lines); (B) change in luminal diameter between post-procedure period and after 6 months in the distal (black lines) and proximal edges (red lines). The green circle represents a patient who developed restenosis at the proximal edge, with significant reduction in luminal areas and diameters. 95% CI: 95% confidence interval.

implanted in 249 lesions in 230 patients. Overall, the higher resolution of OCT identified dissections in 37.8% of treated lesions (26.8% of 395 analyzed edges). In that study, the investigation with OCT was divided into two phases: phase I (September-October 2010, 108 patients and 112 lesions), the OCT was used in all consecutive patients undergoing percutaneous coronary intervention, while in phase II (November 2010 to June 2011, 122 patients and 137 lesions), the OCT was used at the surgeons' discretion, according to their daily practice. In phase I, dissections were identified in 33.9% of treated lesions (25.4% of 181 evaluated edges) representing the true incidence of dissections in edge segments after coronary stenting. In phase II, the incidence of dissections was higher, observed in 40.9% of treated lesions (28% of the 214 evaluated edges), which represents an estimate of what would be expected with the selective use of OCT in situations that the surgeon deemed necessary to complement the investigation with an invasive imaging method (e.g., angiographic haziness in edge segment, step-up/step-down, etc.). Although most (52.8%) dissections were classified as deep (extending to medial or adventitia layer), it is noteworthy that only 16% of the dissections identified by OCT were also visualized by angiography. These figures illustrate the difference in resolution between angiography and invasive imaging methods, such as IVUS and OCT.

In the present study, dissections were identified in 30.7% of 91 analyzed edges after polymeric BRS implantation. Of these, most were superficial (89.3% restricted to intimal/atheroma layer), and none was observed on angiography. Moreover, the distribution of the dissections was similar between the distal and proximal edges of the implanted BRS, contrary to what was previously reported with metallic stents, in which cases the incidence of dissections is usually higher at the distal edge.[10,17] Some technical aspects may explain this discrepancy: (1) in the present study, the treated lesions were less complex, showed less calcification, and were shorter; (2) vessels with large disproportion

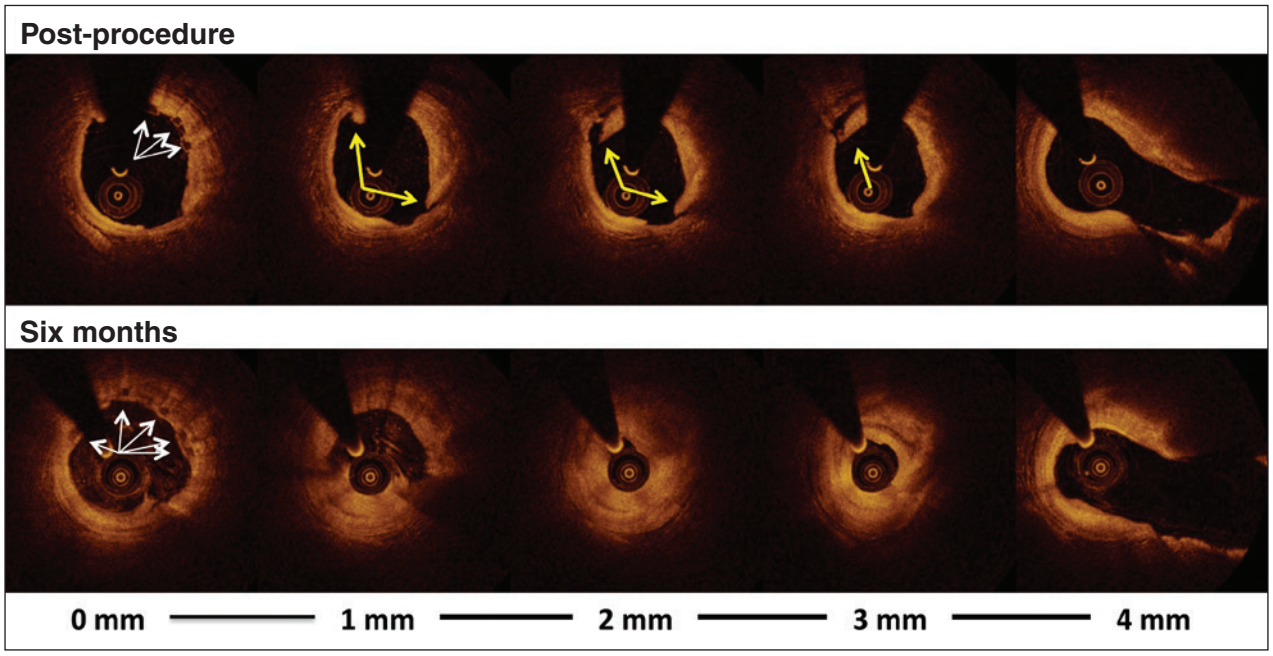

Figure 7 – Case of edge dissection that needed restenosis. Top panel shows cross-sectional images along the 5 mm from the distal edge. The white arrows indicate the bioresorbable scaffold struts positioned over an eccentric fibrotic plaque. Observe the long dissection with coexistence of two flaps (yellow arrows). The bottom panel illustrates cross-sectional images along the 5 mm from the distal edge, corresponding to the regions shown in the top panel. Observe the complete healing of the dissection, but with significant reduction in luminal area, resulting in restenosis. The co-recording of the images acquired post-procedure and after 6 months was possible by using the distances between the bioresorbable scaffold edge and the presence of the large lateral branch in 4 mm.

between the proximal and distal portions were excluded, thus minimizing the risk of injury in the distal segments, which generally have a smaller caliber; (3) per protocol, the implanted BRS should promote full coverage of the lesion by angiography, thus avoiding positioning the device edges on regions with high plaque burden; (4) the post-dilation (when performed) was made with non-compliant balloons, with diameters that were a maximum 0.5 mm larger than the diameter of the implanted BRS, thus avoiding excessive stretching of the device edges; (5) the positioning the post-dilation balloon was generally made on the radiopaque mark on the device, which is located 0.3 mm from the BRS edge, minimizing the risk of balloon inflation outside the BRS limits. Therefore, the technical precision employed and the selection of less complex anatomy may have attenuated the chances of disproportionate injury between the distal and proximal edges, while the effects of the BRS thicker struts acted similarly in both extremities.

Influence of the presence and type of plaque in edge segments

The incomplete coverage of the lesion was associated with increased risk of procedural complications and worse clinical outcome in medium term.[18,19] In a study of 82 edge dissections visualized through IVUS, the eccentricity of the plaque located on the DES edges was identified as an independent predictor for the occurrence of this complication (odds ratio – OR = 1.4; 95% confidence interval – 95% CI: 1.1-1.9; $p = 0.02$).[16] In the analysis of 395 DES edges, the presence of atherosclerotic plaque was identified in 80.7% by OCT, with a significantly higher incidence in edges with dissections (95.3% of dissected edges vs. 75.4% of edges without dissection, $p < 0.001$). Multivariate analysis showed that the presence of atherosclerotic plaque on the edge segment of metallic stents significantly increased the risk of dissections by six-fold (OR = 6.15; 95% CI: 2.09 to 18.11; $p = 0.001$).

Not only the presence of the plaque, but also its characteristics, had great influence on the occurrence of dissections. Although fibrotic plaques were most frequently identified in non-dissected edges, the prevalence of fibrocalcific and lipid-rich plaques was not significantly different between the edges with and without dissection. However, fibrocalcific plaques showed larger circumferential distribution (calcium angle: 125.7 ± 77.9° vs. 65.4 ± 44.3°; $p < 0.001$) and were more superficial (distance of calcium to the lumen: 0.07 ± 0.07 mm vs. 0.15 ± 0.12 mm, $p < 0.001$) in the dissected edges. Lipid-rich plaques located at dissected edges showed thinner fibrous cap (65.9 ± 38.3 µm vs. 103.07 ± 44.6 µm; $p = 0.018$), and greater prevalence of thin-cap fibroatheromas (58.3% vs. 19%; $p = 0.037$) when compared with

lipid-rich plaques in edges without dissections. In the multivariate analysis, positioning the stent edge over a thin-cap fibroatheroma increased the risk of edge dissection by six-fold (OR: 6.16; 95% CI: 1.42 to 26.69; $p = 0.016$). Additional exploratory analysis showed that a minimal fibrous-cap thickness ≤ 80 µm would be the best cut-off for predicting the occurrence of dissections when the stent edges are positioned on a lipid-rich plaque (sensitivity: 73.9%, specificity: 72.5%). Regarding fibrocalcific plaques, their mere presence in the edge segment was not identified as a predictor for dissections. On the contrary, larger circumferential distribution of calcium was an independent predictor of the development of dissections (OR = 1.02 for each increase of 1° in calcium angulation, 95% CI: 1.00 to 1.03; $p = 0.017$). A calcification angle ≥ 72° was identified as the best cut-off for predicting the occurrence of dissections when the stent edges are positioned on a calcified plaque (sensitivity: 73.9%, specificity: 72.5%).[10]

The results of the present study are in agreement with previous data. Among the 28 dissected edges, only one did not have atherosclerotic disease at OCT, in spite of its normal angiographic appearance. In agreement with previous reports, the fibrocalcific plaques were the most prevalent (40.8%), and lipid-rich plaques represented a third (33.3%) of those identified in edge segments. The mean minimal fibrous-cap thickness (145.5 ± 60.4 µm) was considerably higher than that previously reported for the metallic DES;[10] only one lipid-rich plaque met the criteria of thin-cap fibroatheroma. This can be explained by the lower clinical and anatomical complexity of the population included in the present study.

The high prevalence of atherosclerotic disease in the edge segments that appeared normal on the angiogram shows the greater sensitivity of high-resolution invasive methods to identify the disease, but also reinforces the need for a precise technique during the procedure, aiming to minimize the risks of complications. The guide with OCT may be useful in selecting stent dimensions and identifying segments of the vessel with lower risk of dissections, which can be especially important with the larger profile devices, such as polymeric BRS.

Magnitude of edge dissections, evolution, and clinical implications

Vascular injury with plaque rupture can expose its prothrombotic components and lead to acute or subacute thrombosis.[5,6] In fact, edge dissections were associated with increased incidences of thrombosis and MACE.[3-6,20] In general, these dissections are large and associated with more complex angiographic characteristics (type B to F dissections).[3,6,20] Dissimilarly, more superficial, shorter, and less complex dissections that do not limit coronary flow are associated with good clinical outcome.[10,16,17,21]

In the present series of DES edge dissections, the more complex, longer, of higher magnitude, and deeper dissections were treated at the surgeon's discretion. Dissections that were left without further treatment were shorter, less complex, more superficial, and usually observed only on OCT, and had a favorable clinical outcome at the end of one year, similarly to the group of patients treated with DES without edge dissections. As the most severe dissections were treated before hand, the study is insufficient to provide recommendations on which types and sizes of edge dissections are associated with adverse outcomes and should be treated. However, this study indicated some morphometric characteristics that were associated with good clinical outcome and could be managed conservatively, without additional mechanical treatment, namely: longitudinal length < 1.80 mm, less than two concurrent flaps, flap depth ≤ 0.52 mm, flap opening ≤ 0.33 mm, and dissections that do not extend to the medial layer.[10] The dissection characteristics observed in this study meet the above mentioned criteria and corroborate the good clinical evolution observed, with no documented cases of periprocedural infarction or acute/subacute thrombosis.

In the long term, the arterial wall responds to mechanical injury with a series of cellular and molecular mechanisms involved in intimal formation and vascular remodeling, which may, ultimately, lead to restenosis.[22] In the study by Radu et al.,[17] the healing of 22 analyzed dissections occurred favorably, with only two dissections persisting at the end of one year. Interestingly, these two dissections had larger dimensions at the end of the index procedure (lengths of 2.81 and 2.42 mm). No cases of restenosis were documented in this study. In the present study, two cases of dissections persisted after 6 months. The length of one of these dissections (2.7 mm) was similar to that reported by Radu et al.,[17] while the other was considerably longer (4.1 mm). However, both were superficial, restricted to the intimal/atheroma layer of the vessel. Furthermore, significant reductions were observed in the dimensions of these dissections, suggesting an active healing process. The fact that there was no significant reduction in the luminal areas in the edge segments submitted to injury suggests that the dissection healing process is benign, with probable sealing of the flaps, instead of neointimal tissue or plaque material filling the spaces.[8] In fact, only one dissection developed into restenosis and required further intervention. Although this dissection was restricted to the atheroma (Figure 7), it was relatively long (3.8 mm long) and had a more complex morphology, i.e., three flaps visible in the greater injury segment. In the study by Radu et al.[17] and in the present series of edge dissections in DES, the clinical evolution of patients with superficial dissections and small magnitude through OCT was favorable, with no cases of new interventions due to restenosis. The rarity of this outcome in the present population prevents verification of morphometric characteristics that would

be predictive of restenosis or persistence of dissections in medium-term follow-up.

Limitations

The main limitation of the present study was the inclusion of a selected population with low clinical and angiographic complexity. The data related to the incidence and magnitude of edge dissections described herein may thus not represent the actual incidence with the use of polymeric BRS in a population with more complex lesions, more representative of daily clinical practice.

The relatively small number of patients and the low-complexity lesions may be insufficient to detect a significant number of rare events such as acute/subacute thrombosis or edge restenosis in the follow-up period. Therefore, recommendations on which morphometric characteristics would be associated with adverse events and would require treatment cannot be made. However, the present study confirms previous data that small and superficial dissections, only observed through OCT and that do not limit coronary flow, have a good clinical outcome and can be left without further mechanical treatment.

CONCLUSIONS

The incidence of edge dissections by optical coherence tomography after implantation of high-profile polymeric BRS with thicker struts and that require more stringent implantation technique was high (30.7%), but not different from that observed after implantation of metallic DES. These dissections were mostly superficial, of small magnitude, and did not affect coronary flow. None was observed concomitantly with the angiography. Healing was favorable, without significant reduction in luminal dimensions, and 92.8% of dissections were completely resolved after 6 months. No cases of infarction or thrombosis were documented at the in-hospital phase, and only one case of restenosis resulted in new intervention at 6 months. These findings contribute to the body of evidence that small-magnitude dissections that do not limit coronary flow, often seen through high-resolution OCT, have good clinical outcome and can be conducted in a conservative manner, without additional mechanical treatment.

CONFLICTS OF INTEREST

The authors declare no conflicts of interest.

FUNDING SOURCES

None.

REFERENCES

1. Waller BF. "Crackers, breakers, stretchers, drillers, scrapers, shavers, burners, welders and melters"--the future treatment of atherosclerotic coronary artery disease? A clinical-morphologic assessment. J Am Coll Cardiol. 1989;13(5):969-87.
2. Farb A, Virmani R, Atkinson JB, Kolodgie FD. Plaque morphology and pathologic changes in arteries from patients dying after coronary balloon angioplasty. J Am Coll Cardiol.1990;16(6):1421-9.
3. Cutlip DE, Baim DS, Ho KK, Popma JJ, Lansky AJ, Cohen DJ, et al. Stent thrombosis in the modern era: a pooled analysis of multicenter coronary stent clinical trials. Circulation. 2001;103(15):1967-71.
4. Cheneau E, Leborgne L, Mintz GS, Kotani J, Pichard AD, Satler LF, et al. Predictors of subacute stent thrombosis: results of a systematic intravascular ultrasound study. Circulation.2003;108(1):43-7.
5. Rogers JH, Lasala JM. Coronary artery dissection and perforation complicating percutaneous coronary intervention. The J Invasive Cardiol. 2004;16(9):493-9.
6. Biondi-Zoccai GG, Agostoni P, Sangiorgi GM, Airoldi F, Cosgrave J, Chieffo A, et al. Incidence, predictors, and outcomes of coronary dissections left untreated after drug-eluting stent implantation. Eur Heart J. 2006;27(5):540-6.
7. Choi SY, Witzenbichler B, Maehara A, Lansky AJ, Guagliumi G, Brodie B, et al. Intravascular ultrasound findings of early stent thrombosis after primary percutaneous intervention in acute myocardial infarction: a Harmonizing Outcomes with Revascularization and Stents in Acute Myocardial Infarction (HORIZONS-AMI) substudy. Circ Cardiovasc Interv.2011;4(3):239-47.
8. Sheris SJ, Canos MR, Weissman NJ. Natural history of intravascular ultrasound-detected edge dissections from coronary stent deployment. Am Heart J. 2000;139(1 Pt 1):59-63.
9. Bezerra HG, Costa MA, Guagliumi G, Rollins AM, Simon DI. Intracoronary optical coherence tomography: a comprehensive review clinical and research applications. JACC Cardiovasc Interv. 2009;2(11):1035-46.
10. Chamie D, Bezerra HG, Attizzani GF, Yamamoto H, Kanaya T, Stefano GT, et al. Incidence, predictors, morphological characteristics, and clinical outcomes of stent edge dissections detected by optical coherence tomography. JACC Cardiovasc Interv. 2013;6(8):800-13.
11. Holmes DR Jr, Holubkov R, Vlietstra RE, Kelsey SF, Reeder GS, Dorros G, et al. Comparison of complications during percutaneous transluminal coronary angioplasty from 1977 to 1981 and from 1985 to 1986: the National Heart, Lung, and Blood Institute Percutaneous Transluminal Coronary Angioplasty Registry. J Am Coll Cardiol. 1988;12(5):1149-55.
12. TIMI Study Goup. The Thrombolysis in Myocardial Infarction (TIMI) trial. Phase I findings. N Engl J Med. 1985;312(14): 932-6.
13. Tearney GJ, Regar E, Akasaka T, Adriaenssens T, Barlis P, Bezerra HG, et al. Consensus standards for acquisition, measurement, and reporting of intravascular optical coherence tomography studies: a report from the International Working Group for Intravascular Optical Coherence Tomography Standardization and Validation. J Am Coll Cardiol. 2012;59(12):1058-72.
14. Velican D, Velican C. Comparative study on age-related changes and atherosclerotic involvement of the coronary arteries of male and female subjects up to 40 years of age. Atherosclerosis. 1981;38(1-2):39-50.
15. Yabushita H, Bouma BE, Houser SL, Aretz HT, Jang IK, Schlendorf KH, et al. Characterization of human atherosclerosis by optical coherence tomography. Circulation. 2002;106(13):1640-5.
16. Liu X, Tsujita K, Maehara A, Mintz GS, Weisz G, Dangas GD, et al. Intravascular ultrasound assessment of the incidence and predictors of edge dissections after drug-eluting stent implantation. JACC Cardiovasc Interv. 2009;2(10):997-1004.
17. Radu MD, Raber L, Heo J, Gogas BD, Jorgensen E, Kelbaek H, et al. Natural history of optical coherence tomography-detected

non-flow-limiting edge dissections following drug-eluting stent implantation. Euro Intervention. 2014;9(9):1085-94.

18. Lemos PA, Saia F, Ligthart JM, Arampatzis CA, Sianos G, Tanabe K, et al. Coronary restenosis after sirolimus-eluting stent implantation: morphological description and mechanistic analysis from a consecutive series of cases. Circulation.2003;108(3):257-60.
19. Costa MA, Angiolillo DJ, Tannenbaum M, Driesman M, Chu A, Patterson J, et al. Impact of stent deployment procedural factors on long-term effectiveness and safety of sirolimus-eluting stents (final results of the multicenter prospective STLLR trial). Am J Cardiol. 2008;101(12):1704-11.
20. van Werkum JW, Heestermans AA, Zomer AC, Kelder JC, Suttorp MJ, Rensing BJ, et al. Predictors of coronary stent thrombosis: the Dutch Stent Thrombosis Registry. J Am Coll Cardiol. 2009;53(16):1399-409.
21. Kume T, Okura H, Miyamoto Y, Yamada R, Saito K, Tamada T, et al. Natural history of stent edge dissection, tissue protrusion and incomplete stent apposition detectable only on optical coherence tomography after stent implantation – preliminary observation. Circ J. 2012;76(3):698-703.
22. Costa MA, Simon DI. Molecular basis of restenosis and drug-eluting stents. Circulation. 2005;111(17):2257-73.